



HAL
open science

Electrospun Al-MOF fibers as D4 Siloxane adsorbent: Synthesis, environmental impacts, and adsorption behavior

S. Pioquinto-García, J.R. Álvarez, A.A. Rico-Barragán, Sylvain Giraudet,
J.M. Rosas-Martínez, M. Loredó-Cancino, E. Soto-Regalado, V.M.
Ovando-Medina, T. Cordero, J. Rodríguez-Mirasol, et al.

► To cite this version:

S. Pioquinto-García, J.R. Álvarez, A.A. Rico-Barragán, Sylvain Giraudet, J.M. Rosas-Martínez, et al. Electrospun Al-MOF fibers as D4 Siloxane adsorbent: Synthesis, environmental impacts, and adsorption behavior. *Microporous and Mesoporous Materials*, 2023, 348, pp.112327. 10.1016/j.micromeso.2022.112327 . hal-03932166

HAL Id: hal-03932166

<https://hal.science/hal-03932166>

Submitted on 25 Jan 2023

HAL is a multi-disciplinary open access archive for the deposit and dissemination of scientific research documents, whether they are published or not. The documents may come from teaching and research institutions in France or abroad, or from public or private research centers.

L'archive ouverte pluridisciplinaire **HAL**, est destinée au dépôt et à la diffusion de documents scientifiques de niveau recherche, publiés ou non, émanant des établissements d'enseignement et de recherche français ou étrangers, des laboratoires publics ou privés.



Distributed under a Creative Commons Attribution - NonCommercial 4.0 International License

1 Electrospun Al-MOF Fibers as D4 Siloxane
2 Adsorbent: Synthesis, Environmental Impacts,
3 and Adsorption Behavior.

4 *Sandra Pioquinto-García,[†] J. Raziel Álvarez,[†] Alan A. Rico-Barragán,[†] Sylvain Giraudet,[‡]*
5 *Juana María Rosas-Martínez,[§] Margarita Loredó-Cancino,[†] Eduardo Soto-Regalado,[§]*
6 *Tomás Cordero,[§] José Rodríguez-Mirasol^{*§} and Nancy E. Dávila-Guzmán^{*}*

7

8 [†] Facultad de Ciencias Químicas, Universidad Autónoma de Nuevo León, UANL, Av.
9 Universidad S/N, Cd. Universitaria, San Nicolás de los Garza, Nuevo León 66455, Mexico

10 [‡] Ecole Nationale Supérieure de Chimie de Rennes, 11 Allée de Beaulieu, 35708 Rennes,
11 France

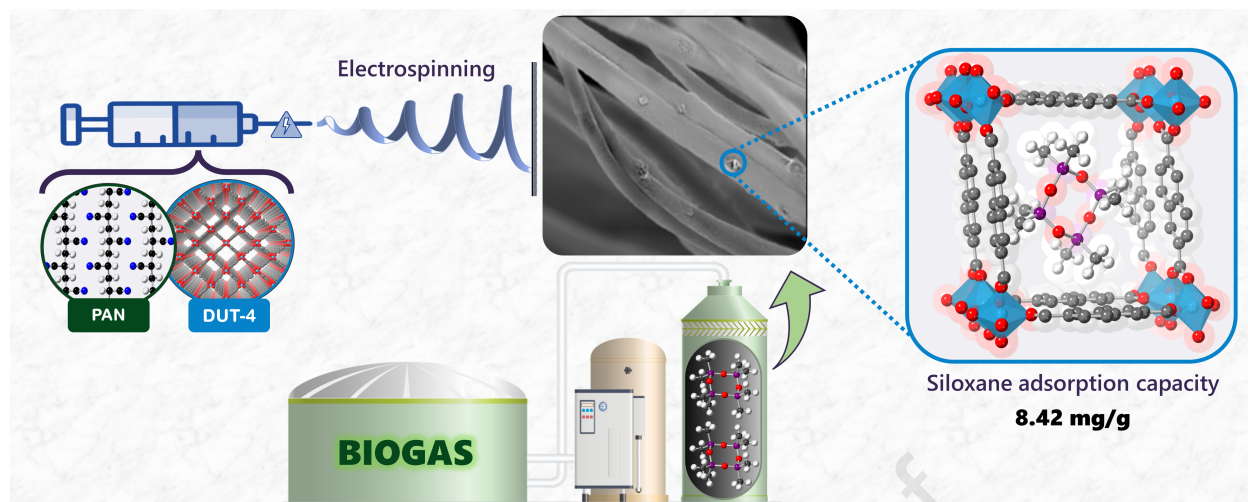
12 [§] Departamento de Ingeniería Química, Universidad de Málaga, Andalucía Tech., Campus
13 de Teatinos s/n, 29010, Málaga, Spain

14 Contact information for the corresponding author (*)

15 Nancy Elizabeth Dávila-Guzmán, Ph. D.

16 Universidad Autónoma de Nuevo León

17 Email: nancy.davilagz@uanl.edu.mx



Journal Pre-proof

18 ABSTRACT

19 Here, we unveil the great potential of metal-organic framework (MOF) composite fibers
20 produced by the electrospinning method to remove D4 siloxane from gaseous solutions.
21 The fibers are based on polyacrylonitrile (PAN) and a microporous aluminum-based MOF
22 known as DUT-4. The electrospinning configuration and DUT-4: PAN ratio in the precursor
23 solutions play an important role in the textural properties of the fibers. Characterizations of
24 morphology and textural properties demonstrated that the best dispersion on the fiber
25 surface was achieved using coaxial electrospinning with a relationship of 1:1.4 of DUT-
26 4: PAN. The Al-MOF fiber composite was evaluated as a D4 siloxane adsorbent, reaching over
27 85% of the D4 siloxane uptake capacity of individual DUT-4 crystals but with faster adsorption
28 kinetics (effective diffusion coefficient 3.31 times higher). In addition, the synthesis of the
29 composite showed a lower environmental impact and better thermal stability than that observed
30 for DUT-4. This work shows the novel DUT-4 fibers have an outstanding potential for
31 siloxane removal from biogas streams.

32

33 *Keywords:* Electrospun, metal-organic frameworks, biogas, octamethylcyclotetrasiloxane

34

35 **1. Introduction**

36 The negotiations to reduce the risks and the impacts of global climate change began in
37 1988 with the creation of the Intergovernmental Panel on Climate Change (IPCC) under the
38 auspices of the World Meteorological Organization (WMO) and the United Nations.
39 Nowadays, each country voluntarily determines what measures are willing to take against
40 climate change and announces them to the rest of the world at the Conference of the Parties

41 (COP).[1] Following the line of sustainable development, the transition from fossil fuels to
42 non-conventional energies (*e.g.*, wind, solar, wave, tidal, or biomass) has been promoted
43 worldwide. One type of renewable energy widely spread is biogas, which can be generated
44 for the anaerobic degradation of residual organic materials by the activity of
45 microorganisms.[2]

46 The biogas is a mixture of methane (55-70%), carbon dioxide (30-45%), moisture,
47 hydrogen sulfide, and volatile organic compounds (VOCs), which may be present in small
48 amounts.[3] Siloxanes can also be formed during the anaerobic fermentation of sewage
49 sludge and organic waste.[4] Siloxanes are a group of Si-based impurities that are
50 considered essential pollutants to remove from biogas.[5] The most abundant siloxanes in
51 biogas are hexamethyldisiloxane (L2), octamethyltrisiloxane (L3), and
52 octamethylcyclotetrasiloxane (D4).[6] They adversely affect biogas combustion systems
53 because they are converted mainly into formaldehyde (CH_2O) and orthosilicic acid
54 (H_4SiO_4), both chemical reagents contribute to abrasion, metal friction, and component
55 failures in machinery.[7]

56 The concentration of siloxanes in biogas from landfills and wastewater treatment plants
57 covers a wide range between 10 mg m^{-3} and a maximum value of up to $2,000 \text{ mg m}^{-3}$. [8]
58 There is no standard specifying the maximum concentration of siloxanes in biogas, but a
59 standard general limit of 15 mg m^{-3} is recommended.[9] The necessity to remove siloxane
60 from biogas is also a priority in order to enhance biogas' energy recovery potential. Current
61 technologies for siloxane removal from biogas include adsorption, absorption, cryogenics,
62 separation by membranes, and biological processes.[10] However, solid-gas adsorption

63 technology has a huge potential due to its low cost, high selectivity, and simple
64 operation.[11]

65 Although solid adsorbents such as activated carbon (AC) or zeolites have been used for
66 siloxane removal, metal-organic frameworks (MOFs) remain promising candidates for this
67 challenging task.[12] MOFs are porous crystalline structures of metal groups joined
68 together by organic ligands. They have high selectivity and feasible recycling/regeneration
69 for biogas purification,[13] mainly due to their large surface area and versatile tunability of
70 their pore environments.[14–16] However, there is still a lack of research attention on using
71 MOFs as platforms for siloxane removal.[17]

72 Mito-oka and coworkers [12] employed three different microporous compounds for
73 siloxane, including DUT-4 (DUT = Dresden University of Technology). DUT-4 is a 3D
74 aluminum-based MOF constructed from a rigid linear 2,6-naphthalenedicarboxylate (2,6-
75 NDC) ligand (Fig. 1). This MOF has the empirical formula $C_{48}H_{28}O_{20}Al_4$, crystallizes in
76 the orthorhombic space group *Pnna*. [18] Its hydrophobic behavior and large BET surface
77 area make DUT-4 an ideal choice for siloxane removal, with a maximum adsorption
78 capacity of 0.5 g g^{-1} . [17] Nevertheless, its poor thermo-mechanical stability, like many
79 other MOFs, is the main obstacle for any real large-scale application. To overcome this
80 problem, several supports have been employed to immobilize powder MOFs with small
81 particle sizes,[19] among which fibers have stood out due to their remarkable properties. In
82 fact, several previous studies have revealed that fibrous structures facilitate the adsorption
83 or catalytic processes.[20–22]

84 Despite all the possible methods currently available for the fabrication of complex fibers,
85 the electrospinning technique remains a simple, versatile, and cost-effective method to
86 manufacture them.[23] Ostermann *et al.* [24] prepared fibers of MOF for the first time by
87 electrospinning, obtaining a hierarchical MOF fiber with a high surface area and easy
88 accessibility. On top of that, the thermal decomposition temperature was enhanced after
89 incorporating the electrospun fibers in a Cr-MOF.[25] Bearing these considerations in
90 mind, functionalized fibers with MOF could be a viable option to remove siloxanes because
91 of their selectivity in wet conditions, renewability at low temperatures (< 300 °C), and
92 reusability. However, to the best of our knowledge, studies of electrospun fibers for
93 applications in biogas purification processes using MOF have not been reported before. For
94 this reason, the present work presents the preparation of DUT-4 electrospun fibers by
95 dissolution methods to improve their adsorption properties of siloxane D4.

96 **2. Materials and methods**

97 *2.1. Preparation of electrospun solutions*

98 The Al-MOF fibers were prepared using DUT-4, *N, N*-dimethylformamide (DMF), and
99 polyacrylonitrile (PAN, $M_w \sim 150,000$ g/mol) solutions. DUT-4 was synthesized according
100 to the procedures previously described [26]; DMF and PAN were purchased from Sigma-
101 Aldrich and used as received without further purification. The solutions were sonicated for
102 up to 4 h to obtain a homogeneous DUT-4 dispersion on the surface of electrospun fibers
103 and MOF particles smaller than 100 nm. The homogeneous suspensions for uniaxial
104 electrospinning were composed of solutions 1 and 2 (see Table 1). Previously, each
105 solution was prepared at 350 rpm for about 1 h but held at different temperatures (solution

106 1 at 80 °C and solution 2 at room temperature). Additionally, solution 2 was sonicated for
107 40-50 min. Preparation conditions of the homogeneous suspensions for the coaxial
108 electrospinning process (detailed in ESI) were the same as the uniaxial solutions 1 and 2,
109 but without mixing them.

110 *2.2. Fiber electrospinning*

111 Purpose-built electrospinning equipment was employed for fibers preparation (see ESI).
112 The solution in the shell (solution 2, electrospinning coaxial), which contained the DUT-4,
113 had to carry PAN to give it greater viscosity and prevent the particles from being projected
114 toward the collector. Milliliter by milliliter was also spun to prevent the particles from
115 precipitating into the syringe. In the uniaxial conditions, the needle was set at 20 cm from
116 the aluminum plate with a flow rate of 2.2 mL/h. The applied electrical potential difference
117 to produce fibers was 20 kV (tips at +10 kV and collector potential at -10 kV). The coaxial
118 conditions for both syringes were a flow rate of 0.9 mL/h, a distance of 23 cm, and an
119 electrical potential difference was 20 kV. The fibers were stabilized at 120 °C.

120 *2.3. Characterization of the Fibers*

121 The surface area and porosity of DUT-4 powders and fibers were determined by N₂
122 adsorption-desorption at -196 °C (77 K), performed in a Micromeritics ASAP 2020
123 apparatus. Samples were outgassed at 150 °C for at least 8 h. From the N₂ isotherm, the
124 apparent surface area (S_{BET}) was determined by applying the Brunauer, Emmett, and Teller
125 (BET) equation.[27] In addition, micropore volume (V_{mp}) and external surface area (S_{t})
126 were calculated by the t -plot method;[28] mesopore volume (V_{mes}) was obtained as the
127 difference between the pore volume (V_{p}) assessed at a relative pressure close to unity (P/P_0)

128 ≈ 0.995) and the micropore volume.[29] To estimate the amount of DUT-4 in grams
 129 accessible into the fibers from the S_{BET} , the following equation was used:[30]

$$130 \quad m_{DUT-4 \text{ on fiber}} = \frac{S_{BET}(DUT-4+fiber) - S_{BET}(PAN \text{ fiber})}{S_{BET}(DUT-4)} \quad 1$$

131 Scanning electron microscopy (SEM) images were obtained using a JEOL JSM-6490LV
 132 microscope with acceleration voltage from 0.3 to 30 kV and a thermionic electron gun with
 133 W filament. Fourier transform infrared (FTIR) spectra were obtained from a Bruker Tensor
 134 27 using a Golden Gate single-reflection diamond attenuated total reflection (ATR) cell to
 135 identify the functional groups on the fibers' surface, a standard spectral resolution of 4 cm^{-1}
 136 in the spectral range of 4000 to 500 cm^{-1} , were carried out. Powder X-ray diffraction
 137 (PXRD) patterns were collected in Bragg-Brentano geometry with $\text{Cu-K}\alpha$ ($\lambda = 1.54060 \text{ \AA}$)
 138 monochromatized radiation on a PANalytical X'Pert PRO diffractometer operating with an
 139 intensity of 40 mA and a tension of 45 kV. The instrument was equipped with an
 140 X'Celerator RTMS (real-time multiple-strip) detector, and the sample patterns were
 141 recorded from 5 to 80° (2θ). Thermogravimetric analysis (TGA) was performed with a
 142 TGA 500 (TA Instruments Ltd., UK) using sample sizes of 7 to 14 mg at a heating rate of
 143 $20 \text{ }^\circ\text{C}/\text{min}$ from room temperature to $800 \text{ }^\circ\text{C}$ under an N_2 atmosphere.

144 *2.4. Green Assessment*

145 To quantitatively assess the greenness of DUT-4 and 70DUT-4@PAN, the free web-
 146 based DOZNTM 2.0 evaluator by MilliporeSigma was employed.[31] The software
 147 calculates the environmental impact by taking a count of the properties of raw materials,
 148 such as chemicals and solvents, including system values, such as temperature and

149 pressure.[32] The data was recollected using the UN's Globally Harmonized System of
150 Classification and Labelling of Chemicals (GHS) and Security Data Sheet (SDS). The input
151 data of temperature, time, pressure, and raw materials used for DOZNTM 2.0 are listed in
152 ESI.

153 *2.5. Adsorption experiments*

154 The adsorption experiments were carried out at 450 mg/Nm³ of initial concentration of
155 D4, 100 mg of adsorbent material, and room temperature. The mixtures were stirred at 700
156 rpm for 6–9 h to ensure equilibrium. The D4 concentration of samples was determined by
157 gas chromatography with a flame ionization detector (GC-FID) using a Shimadzu Nexis
158 GC-2030 (Shimadzu Corp., Kyoto, Japan). A Shimadzu SH-Rxi-5ms capillary column
159 (15 m x 0.25 mm inner diameter x 0.25 µm film thickness) was employed. The GC-FID
160 operational conditions were oven temperature at 110 °C; detector temperature, 250 °C; inlet
161 temperature, 150 °C (at 83.3 kPa); carrier gas, He at a flow rate of 1.5 mL min⁻¹; splitting
162 ratio, 5.0. An injection volume of 0.5 mL was employed with a total method duration of 1.4
163 min. The adsorption capacity was calculated using the mass balance in the following way:

$$164 \quad q_e = \frac{(C_0 - C_e)V}{m} \quad 2$$

165 where q_e is the adsorption capacity (mg/g), C_0 and C_e represent the initial and equilibrium
166 concentration of D4 (mg/Nm³), V is the volume of D4 solution (m³), and m is the mass of
167 the adsorbent (g).

168 *2.6. Kinetic modeling*

169 It is generally known that the adsorption kinetics of porous materials is controlled by
 170 intraparticle diffusion.[33] The homogeneous solid diffusion model (HSDM) is a typical
 171 intraparticle diffusion model, the equation is as follows:

$$172 \quad \frac{\partial q}{\partial t} = \frac{D}{r^2} \frac{\partial}{\partial r} \left(r^2 \frac{\partial q}{\partial r} \right) \quad 3$$

173 Crank gave an exact solution to the HSDM model for the case of constant concentration
 174 at the surface (known as "infinite bath"), negligible external film resistance, and spherical
 175 adsorbent particles initially free of solute.[34] Crank's model is as follows:

$$176 \quad \frac{q}{q_e} = 1 - \frac{6}{\pi^2} \sum_{n=1}^{\infty} \frac{1}{n^2} e^{\left(-\frac{Dn^2\pi^2 t}{R^2} \right)} \quad 4$$

177 where q and q_e are the adsorption capacity at any time and at equilibrium, respectively
 178 (mg/g); D is the effective diffusion coefficient (m^2/h), t is the time (h), and R is the particle
 179 radius (m). This model was used to describe the kinetics of D4 siloxane onto DUT-4
 180 powder and DUT-4 fibers and to obtain the effective diffusion coefficients.

181 In addition, well-known adsorption kinetics models, the pseudo-first-order model (PS-1)
 182 and the pseudo-second-order model (PS-2), were tested for the D4 siloxane adsorption, and
 183 the equations are presented as follows:

$$184 \quad q = q_e (1 - e^{-K_1 t}) \quad 5$$

$$185 \quad q = \frac{K_2 q_e^2 t}{1 + K_2 q_e t} \quad 6$$

186 where q and q_e are the adsorption capacity at any time and equilibrium, respectively
 187 (mg/g); K_1 and K_2 are the rate constants for the PS-1 and PS-2 models (h^{-1}), respectively,

188 and t is the time (h). The kinetic model parameters were obtained by non-linear regression
189 minimizing the standard error (Eq. 7) using the Solver add-in tool of Microsoft Excel®.
190 The goodness of fitting results was determined by the coefficient of determination (R^2).

$$191 \quad SE = \sqrt{\frac{\sum_{i=1}^n (q_{exp} - q_{cal})^2}{n-k}} \quad 7$$

192 **3. Results and discussion**

193 *3.1. Textural properties of the fibers*

194 The BET surface area of activated DUT-4 was estimated to be 1,655 m²/g (ESI) and falls
195 well with previously reported data for this MOF.[17] The nitrogen adsorption-desorption
196 isotherms obtained at -196 °C of the different DUT-4 fibers prepared by electrospinning are
197 type I, associated with microporous solids, independently of the electrospinning
198 configuration used (Fig. 2). These isotherms are characterized by a significant nitrogen
199 uptake at very low relative pressures. In the case of uniaxial configuration, the low volume
200 of nitrogen adsorbed at relative pressures below 0.1 shows only a limited increase of this
201 compared to the volume of nitrogen adsorbed by the PAN fiber without DUT-4. In contrast,
202 using a coaxial configuration considerably increases the volume of nitrogen adsorbed, and
203 this adsorption is directly related to the amount of DUT-4 added to the spinnable solution.
204 In addition, this coaxial configuration can also show a significant increase in the volume of
205 nitrogen adsorbed at high relative pressures, evidencing the further presence of larger
206 mesopores. Therefore, this configuration can produce DUT-4 fibers with a hierarchical
207 bimodal porous structure.

208 Table 2 collects the corresponding textural properties derived from the nitrogen
209 adsorption-desorption isotherms obtained at -196 °C of the DUT-4 fibers prepared by
210 electrospinning at different configurations and experimental conditions. The coaxial
211 configuration allowed to include not only higher amounts of DUT-4 but also reached
212 continuous fibers with apparent surface areas as high as $\sim 300 \text{ m}^2/\text{g}$. In this sense, S_{BET}
213 values increased from 37 to 293 m^2/g as the ratio of DUT-4 to PAN enhanced; meanwhile,
214 pore volumes, mainly associated with mesopore volumes, varied from 0.1 to 0.36 cm^3/g ,
215 suggesting the dual formation of micro and large mesopores.

216 The use of other solvents different than DMF was also analyzed. The calculated S_{BET} was
217 lower for the fibers prepared with DMSO. Specifically, S_{BET} was halved with uniaxial
218 electrospinning, while in coaxial electrospinning, S_{BET} was reduced up to four times using
219 DMSO, so its use was discarded. Finally, it is important to highlight that although the
220 specific surface area increases with the amount of DUT-4 added to the solution, SEM
221 images (*vide infra*) showed DUT-4 particles of sizes larger than 1 μm on the surface of the
222 fibers, so to optimize the dispersion of the DUT-4 particles, the use of solutions with DUT-
223 4 percentages higher than 70% were not advisable.

224 From equation 1, the mass of DUT-4 accessible by nitrogen was calculated. For fibers
225 obtained by coaxial electrospinning, the $m_{\text{DUT-4 on fiber}} (\text{g})$ increases following the next
226 order: 20DUT-4@PAN (0.016) < 70DUT-4@PAN (0.062) < 100DUT-4@PAN (0.073) <
227 140DUT-4@PAN (0.170). However, these values represent a fraction of the initial amount
228 of MOF on the electrospinning solution. For example, for 70DUT-4@PAN fiber, only 25%

229 of the initial DUT-4 mass is accessible by nitrogen suggesting the MOF is highly
230 embedded into fibers with the formation of a thin PAN barrier coating DUT-4 particles.[35]

231 3.2. SEM images

232 Scanning electron microscopy was used to select the type of fibers that presented the best
233 distribution of DUT-4 on the fiber surface. In Fig. 3, it can be observed that the diameters
234 of the fibers obtained by coaxial electrospinning showed smaller diameters than those
235 obtained by uniaxial electrospinning. The diameters for 20DUT-4@PAN, 70DUT-4@PAN,
236 100DUT-4@PAN, and 140DUT-4@PAN fibers were from 0.125 μm to 0.5 μm . In these
237 types of fibers, it shows that as the amount of DUT-4 increased in the spinnable solution
238 (*i.e.*, 20DUT-4@PAN < 70DUT-4@PAN < 100DUT-4@PAN < 140DUT-4@PAN), more
239 particles were seen on the surface of the fiber. Furthermore, at higher DUT-4 loading
240 fractions, particle agglomeration was observed. As a result, DUT-4 agglomerates (with an
241 overall size >1.0 μm) were trapped between a set of fibers. Therefore, the fibers generated
242 by 70DUT-4@PAN coaxial electrospinning had the best dispersion on the fiber surface
243 without trapping problems.

244 3.3. Thermal and structural characterization of the electrospun fibers

245 FTIR studies of fibers are an important characterization technique to identify the
246 functional groups on the surface material, which could be useful to explain the adsorption
247 process on the adsorbent material. In Fig. 4, the FTIR spectra of 70DUT-4@PAN and PAN
248 fibers are shown, the band observed at 1617.33 cm^{-1} corresponds to asymmetric stretching
249 vibrations of the group $\nu_{as}(\text{C}-\text{O})$, [36] the band at 991.40 cm^{-1} is associated with the
250 bending of bridging groups $\delta(\text{OH})$, [37] besides the 792.08 cm^{-1} band is related to flexions

251 into the aromatic plane;[38] the bands at 1440.69 and 1364.55 cm^{-1} can be assigned to the
252 symmetric $\nu_s(\text{OCO})$ stretching vibration of carboxylate group while the observed bands
253 from 570.48 to 502.26 cm^{-1} could be associated to the stretching vibrations of the Al–O
254 bond, in good agreement with previously reported data.[36]

255 To investigate the relation between PAN and DUT-4 particles in the electrospun
256 composite fibers, PXRD measurements were performed (Fig. 5). The PXRD pattern of an
257 as-synthesized sample of DUT-4 showed three characteristic reflections for this MOF ($2\theta =$
258 6.9, 13.9, and 21.0°) corresponding to the hkl Miller index (101), (011), and (303). For
259 polyacrylonitrile (PAN) fibers, the PXRD pattern shows an intense reflection (110) plane at
260 $2\theta = 16.8^\circ$ and a weak one located at $2\theta = 29.3^\circ$ due to the (020) lattice plane of PAN.[39]
261 On the other hand, the broad reflection at $2\theta \approx 25^\circ$ was related to the (002) planes. These
262 reflections are in agreement with a hexagonal chain packing of electrospun PAN-based
263 fibers.[40] Finally, in the PXRD of 70DUT-4@PAN fibers, the characteristic diffraction
264 peaks of both PAN and DUT-4 were observed. Therefore, the successful introduction of
265 DUT-4 into PAN fibers can be confirmed. The two most intense reflections of DUT-4,
266 which are related to the inorganic portion of the framework (*i.e.*, Al^{3+} distorted octahedral
267 positions), were superimposed on the broad reflection and uneven baseline of PAN,
268 suggesting that DUT-4 exists as crystalline material in the 70DUT-4@PAN composite.

269 Fig. 6(a) and 6(b) show the TGA thermograms and their derivatives of PAN fiber and
270 70DUT-4@PAN, respectively. For pure PAN fibers, a lower amount of absorbed water is
271 observed at 100 °C (approximately 2.5%), and then two important weight losses can be
272 seen. The first between 200 and 310 °C, centered at 282 °C with 30% of weight loss, and

273 the second change between 312 and 500 °C, centered at 430 °C representing 32% of weight
274 loss, giving a total weight loss of 68% at 800 °C (excluding absorbed water). The TGA
275 curve of PAN fibers has the typical thermal stability and weight loss percentages for this
276 polymer. It has been reported that thermal changes of PAN fibers depend on the thermal
277 processing during its manufacture (*i.e.*, stabilization temperature and processing time). If
278 PAN was stabilized for short periods and at relatively low temperatures, a change is usually
279 observed at 300 °C, indicating cyclization reactions with volatile gases coming out. At
280 higher temperatures, between 320 and 480 °C, a second thermal change is typically
281 observed and is related to a dehydrogenation reaction. Finally, in the last stage, until
282 700 °C, the total weight loss decreased monotonously to approximately 63%.[41] On the
283 other hand, the sample of 70DUT-4@PAN presented higher thermal stability than alone
284 PAN fibers with the observed changes for PAN fibers but with shifting at higher
285 temperatures due to the presence of DUT-4, hindering chain mobility, with the first change
286 centered at 321 °C and the second to 532 °C. However, a new change was detected at 600
287 °C ascribed to partial degradation of DUT-4, to give a total degradation up to 800 °C of
288 ~64% (*i.e.*, 4% less than alone PAN fibers).

289 3.4. Quantitative Green Chemistry Evaluation

290 In addition to all physicochemical analyses, a comprehensive assessment of the
291 environmental impact of fiber fabrication was conducted. According to green chemistry,
292 the ideal chemical synthesis or manufacturing eliminates or reduces the waste generated,
293 uses a negligible amount of energy, and produces no harmful products.[31] Herein, an open
294 software (DOZNTM) was used to assess the compliance with green chemistry principles
295 (GCP) of DUT-4 and 70DUT-4@PAN (Fig. 7). Values near 0 express a minimal effect on

296 GCP; meanwhile, high values indicate a negative influence on GCP.[42] Minor impacts of
297 synthesis were found in **GCP 4** (designing safer chemicals), and no significant differences
298 were found in **GCP 8** (reduce derivatives), **GCP 9** (catalysis), and **GCP 11** (real-time
299 analysis for pollution prevention). A major part of the impact of Principles of Green
300 Chemistry due production of fibers was related to DUT-4 synthesis; for example, in **GCP 1**
301 (waste prevention), the environmental score referred to DUT-4 was near 500, meanwhile,
302 70DUT-4@PAN was 40. Although DUT-4 synthesis and 70DUT-4@PAN used DMF as a
303 solvent, the mass needed in synthesis was higher (28.32 g) than fibers production (6 g), and
304 the value obtained in **GCP 1** was mainly affected by the waste severity of DMF.[31] The
305 90% of impacts observed in **GCP 1, GCP 2, GCP 3, GCP 5, GCP 6, GCP 7, GCP 10,**
306 **and GCP 12** were produced in DUT-4 synthesis due to the waste toxic solvent. According
307 to DOZNTM, DUT-4 has an environmental score of 66, higher than the score of 1 for the
308 fabrication of 70DUT-4@PAN fibers.

309 3.5. Siloxane Adsorption Performance

310 The adsorption experiments were carried out at an initial concentration of 450 mg/Nm³ of
311 siloxane D4 at room temperature. This concentration was used to be consistent with the
312 values found in real biogas streams (*i. e.*, at low loadings). The kinetics for the adsorption
313 of D4 was rapid, reaching equilibrium at about 3~3.5 h (Fig. 8). The adsorption capacity of
314 the PAN fibers was tiny, 0.86 mg/g at the equilibrium concentration of 403.27 mg/m³. The
315 adsorption capacity for the coaxial electrospun fibers was increased from 4.13 to 8.42 mg/g
316 at an equilibrium concentration of 256.85 to 61.26 mg/m³, respectively.

317 In this sense, the fibers with the highest siloxane adsorption capacity were those
318 electrospun coaxially, which are the fibers with the highest DUT-4 powder load and,

319 therefore, the highest S_{BET} . Although, the relationship between the siloxane adsorption
320 capacity and the specific surface area was not linear (Fig. S4). The materials obtained by
321 coaxial electrospinning achieved slight differences in the adsorption capacity. In addition,
322 the adsorption capacities obtained by coaxial fibers were only 15% lower than the DUT-4
323 powder. However, the diffusion of D4 onto coaxial fibers 20DUT-4@PAN and 70DUT-
324 4@PAN was 2.9 and 3.31-fold higher than on DUT-4 powder, based on the effective
325 diffusion coefficients obtained from Crank's model (Fig. 9). These results indicate that
326 MOF particles are fully accessible inside the polymeric fibers and that the particle
327 distribution on coaxial fibers favors the contact between the D4 siloxane and MOF
328 particles.

329 The kinetic data were fitted by the pseudo-first-order model (PS-1), pseudo-second-order
330 model (PS-2), and Crank model. The calculated model parameters and their suitability to
331 represent experimental data are shown in Table 3. Based on the high determination
332 coefficient (R^2), the kinetic adsorption of D4 on DUT-4 nanofibers can be best represented
333 by the Crank model, a well-known kinetics model based on intraparticle diffusion. These
334 results suggest that the adsorption of D4 on DUT-4 nanofibers is controlled by internal
335 mass transfer resistance, which is the common rate-limiting step for porous adsorbent
336 materials.[43]

337 Finally, the adsorption cyclability of D4 siloxane from 70DUT-4@PAN fibers by thermal
338 treatment was evaluated (see Fig. S6). For this material, a low regeneration time (~ 4 h)
339 was employed. Although the fibers kept their adsorption capacity showing good
340 repeatability, the complete regeneration of material under mild conditions was not
341 achieved. This behavior can be attributed to the strong interaction between D4 siloxane and

342 the composite fibers. The FTIR spectra of 70DUT-4@PAN before and after D4 siloxane
343 adsorption were performed to clarify some aspects of the adsorption processes (Fig. S7).
344 The methyl groups of the voluminous D4 molecule are expected to be mainly responsible
345 for the adsorption complex formation. Due to this, the δ (Si-CH₃) band shifts to higher
346 wavenumbers up to 1290 cm⁻¹. On the other hand, the Si-O-Si stretching band shifts to
347 1142 cm⁻¹. In comparison with pure D4 siloxane,[44] the position of absorption bands
348 suggests a confinement effect. Due to the adsorption process, the material shows absorption
349 bands with greater intensities than the original spectrum of 70DUT-4@PAN. This behavior
350 could be attributed to the increase in the bond polarity of the functional groups of DUT-4 as
351 a result of the strong interaction with D4 siloxane.

352 **4. Conclusions**

353 In summary, a novel composite from PAN and Al-MOF was successfully synthesized via
354 electrospinning and can be used as an adsorbent to remove D4 siloxane for biogas
355 purification applications. The coaxial electrospinning technique produced fibers with a
356 hierarchical bimodal porous structure and superior textural characteristics compared to the
357 uniaxial technique. Furthermore, the Al-MOF particles were well dispersed by coaxial
358 electrospinning and were fully accessible inside the polymeric fibers. For this reason, fast
359 adsorption kinetics was achieved (3.5 h), and the diffusion of D4 siloxane molecules was
360 enhanced compared to DUT-4 powder. Moreover, the production of PAN fibers with DUT-
361 4 by coaxial electrospinning had lower environmental impacts than the synthesis of the
362 DUT-4 powder due to its low Al-MOF loadings. Taking advantage of the low
363 environmental burden of the electrospun PAN@DUT-4 fibers and its fast kinetics, the

364 novel composite proposed could be of interest for the removal of D4 siloxane from gaseous
365 solutions.

366 **CRedit authorship contribution statement**

367 **Sandra Pioquinto-García:** Conceptualization, Formal analysis, Data curation,
368 Investigation. **J. Raziél Álvarez:** Formal analysis, Data curation, Writing – review &
369 editing. **Alan A. Rico-Barragán:** Data curation, Formal analysis. **Sylvain Giraudet:**
370 Formal analysis, Writing – review & editing. **Juana María Rosas-Martínez:**
371 Methodology, Formal Analysis. **Margarita Loredo-Cancino:** Validation, Formal analysis.
372 **Eduardo Soto-Regalado:** Writing – review & editing, Formal analysis. **Tomás Cordero:**
373 Formal analysis, Methodology. **José Rodríguez-Mirasol:** Conceptualization, Project
374 administration, Funding acquisition. **Nancy E. Dávila-Guzmán:** Conceptualization,
375 Writing – review & editing, Resources, Project administration, Funding acquisition.

376 **Declaration of Competing Interest**

377 The authors declare that they have no known competing financial interests or personal
378 relationships that could have appeared to influence the work reported in this paper.

379 **Acknowledgments**

380 This research was supported by Facultad de Ciencias Químicas and Consejo Nacional de
381 Ciencia y Tecnología de Mexico (Scholarship number 781451). J. R. Á. acknowledges
382 CONACYT for the postdoctoral fellowship (“Estancias Posdoctorales por México-2021”);
383 thanks also to J. J. Romero and R. M. Romero for many valuable discussions.

384 **Appendix A. Supplementary data**

385 Supplementary data to this article can be found online

386 Details of the electrospinning setup, precursor solutions, BET plots and t-plots of fibers
387 samples, and the relationship between BET surface area and D4 adsorption capacity (PDF).

388 Input and output data from global greenness evaluation using DOZNTM (XLSX).

389 **References**

- 390 [1] S.N. Seo, Beyond the Paris Agreement: Climate change policy negotiations and
391 future directions, *Reg. Sci. Policy Pract.* 9 (2017) 121–140.
392 <https://doi.org/10.1111/rsp3.12090>.
- 393 [2] K. Oibileke, N. Nwokolo, G. Makaka, P. Mukumba, H. Onyeaka, Anaerobic
394 digestion: Technology for biogas production as a source of renewable energy—A
395 review, *Energy Environ.* 32 (2021) 191–225.
396 <https://doi.org/10.1177/0958305X20923117>.
- 397 [3] O.W. Awe, Y. Zhao, A. Nzihou, D.P. Minh, N. Lyczko, A Review of Biogas
398 Utilisation, Purification and Upgrading Technologies, *Waste and Biomass*
399 *Valorization.* 8 (2017) 267–283. <https://doi.org/10.1007/s12649-016-9826-4>.
- 400 [4] G. Wang, Z. Zhang, Z. Hao, Recent advances in technologies for the removal of
401 volatile methylsiloxanes: A case in biogas purification process, *Crit. Rev. Environ.*
402 *Sci. Technol.* 49 (2019) 2257–2313.
403 <https://doi.org/10.1080/10643389.2019.1607443>.

- 404 [5] X.Y. Chen, H. Vinh-Thang, A.A. Ramirez, D. Rodrigue, S. Kaliaguine, Membrane
405 gas separation technologies for biogas upgrading, *RSC Adv.* 5 (2015) 24399–24448.
406 <https://doi.org/10.1039/C5RA00666J>.
- 407 [6] L. Ghorbel, R. Tatin, A. Couvert, Relevance of an organic solvent for absorption of
408 siloxanes, *Environ. Technol.* 35 (2014) 372–382.
409 <https://doi.org/10.1080/09593330.2013.828778>.
- 410 [7] J. Álvarez-Flórez, E. Egusquiza, Analysis of damage caused by siloxanes in
411 stationary reciprocating internal combustion engines operating with landfill gas, *Eng.*
412 *Fail. Anal.* 50 (2015) 29–38. <https://doi.org/10.1016/j.engfailanal.2015.01.010>.
- 413 [8] T. Jiang, W. Zhong, T. Jafari, S. Du, J. He, Y.-J. Fu, P. Singh, S.L. Suib, Siloxane
414 D4 adsorption by mesoporous aluminosilicates, *Chem. Eng. J.* 289 (2016) 356–364.
415 <https://doi.org/10.1016/j.cej.2015.12.094>.
- 416 [9] M. Schweigkofler, R. Niessner, Removal of siloxanes in biogases, *J. Hazard. Mater.*
417 83 (2001) 183–196. [https://doi.org/10.1016/S0304-3894\(00\)00318-6](https://doi.org/10.1016/S0304-3894(00)00318-6).
- 418 [10] M. Ajhar, M. Travesset, S. Yüce, T. Melin, Siloxane removal from landfill and
419 digester gas – A technology overview, *Bioresour. Technol.* 101 (2010) 2913–2923.
420 <https://doi.org/10.1016/j.biortech.2009.12.018>.
- 421 [11] W. Xing, Q. Liu, J. Wang, S. Xia, L. Ma, R. Lu, Y. Zhang, Y. Huang, G. Wu, High
422 Selectivity and Reusability of Biomass-Based Adsorbent for Chloramphenicol
423 Removal, *Nanomaterials.* 11 (2021) 2950. <https://doi.org/10.3390/nano11112950>.

- 424 [12] Y. Mito-oka, S. Horike, Y. Nishitani, T. Masumori, M. Inukai, Y. Hijikata, S.
425 Kitagawa, Siloxane D4 capture by hydrophobic microporous materials, *J. Mater.*
426 *Chem. A.* 1 (2013) 7885–7888. <https://doi.org/10.1039/c3ta11217a>.
- 427 [13] A. Peluso, N. Gargiulo, P. Aprea, F. Pepe, D. Caputo, Nanoporous Materials as H₂S
428 Adsorbents for Biogas Purification: a Review, *Sep. Purif. Rev.* 48 (2019) 78–89.
429 <https://doi.org/10.1080/15422119.2018.1476978>.
- 430 [14] T. Saeed, A. Naeem, I. Ud Din, M.A. Alotaibi, A.I. Alharthi, I. Wali Khan, N. Huma
431 Khan, T. Malik, Structure, nomenclature and viable synthesis of micro/nanoscale
432 metal organic frameworks and their remarkable applications in adsorption of organic
433 pollutants, *Microchem. J.* 159 (2020) 105579.
434 <https://doi.org/10.1016/j.microc.2020.105579>.
- 435 [15] M. Sánchez-Serratos, J.R. Álvarez, E. González-Zamora, I.A. Ibarra, Porous
436 Coordination Polymers (PCPs): New Platforms for Gas Storage, *J. Mex. Chem.*
437 *Soc.* 60 (2016) 43–57.
- 438 [16] L. Öhrström, Let's talk about MOFs—Topology and terminology of metal-organic
439 frameworks and why we need them, *Crystals.* 5 (2015) 154–162.
440 <https://doi.org/10.3390/cryst5010154>.
- 441 [17] E. Gulcay, P. Iacomì, Y. Ko, J.S. Chang, G. Rioland, S. Devautour-Vinot, G.
442 Maurin, Breaking the upper bound of siloxane uptake: metal–organic frameworks as
443 an adsorbent platform, *J. Mater. Chem. A.* 9 (2021) 12711–12720.
444 <https://doi.org/10.1039/D1TA02275J>.

- 445 [18] I. Senkovska, F. Hoffmann, M. Fröba, J. Getzschmann, W. Böhlmann, S. Kaskel,
446 New highly porous aluminium based metal-organic frameworks: Al(OH)(ndc) (ndc
447 = 2,6-naphthalene dicarboxylate) and Al(OH)(bpdc) (bpdc = 4,4'-biphenyl
448 dicarboxylate), *Microporous Mesoporous Mater.* 122 (2009) 93–98.
449 <https://doi.org/10.1016/j.micromeso.2009.02.020>.
- 450 [19] J.E. Efome, D. Rana, T. Matsuura, C.Q. Lan, Insight Studies on Metal-Organic
451 Framework Nanofibrous Membrane Adsorption and Activation for Heavy Metal
452 Ions Removal from Aqueous Solution, *ACS Appl. Mater. Interfaces.* 10 (2018)
453 18619–18629. <https://doi.org/10.1021/acsami.8b01454>.
- 454 [20] K.-L. Chiu, F. Kwong, D.H.L. Ng, Enhanced oxidation of CO by using a porous
455 biomorphic CuO/CeO₂/Al₂O₃ compound, *Microporous Mesoporous Mater.* 156
456 (2012) 1–6. <https://doi.org/10.1016/j.micromeso.2012.02.015>.
- 457 [21] K.-L. Chiu, D.H.L. Ng, Synthesis and characterization of cotton-made activated
458 carbon fiber and its adsorption of methylene blue in water treatment, *Biomass and
459 Bioenergy.* 46 (2012) 102–110. <https://doi.org/10.1016/j.biombioe.2012.09.023>.
- 460 [22] Z. Zhang, J. Li, F. Sun, D. H. L. Ng, F. Kwong, S. Liu, Preparation and
461 Characterization of Activated Carbon Fiber from Paper, *Chinese J. Chem. Phys.* 24
462 (2011) 103–108. <https://doi.org/10.1088/1674-0068/24/01/103-108>.
- 463 [23] D. Han, A.J. Steckl, Coaxial Electrospinning Formation of Complex Polymer Fibers
464 and their Applications, *Chempluschem.* 84 (2019) 1453–1497.
465 <https://doi.org/10.1002/cplu.201900281>.

- 466 [24] R. Ostermann, J. Cravillon, C. Weidmann, M. Wiebcke, B.M. Smarsly, Metal-
467 organic framework nanofibers via electrospinning, *Chem. Commun.* 47 (2011) 442–
468 444. <https://doi.org/10.1039/c0cc02271c>.
- 469 [25] J. Ren, N.M. Musyoka, P. Annamalai, H.W. Langmi, B.C. North, M. Mathe,
470 Electrospun MOF nanofibers as hydrogen storage media, *Int. J. Hydrogen Energy.*
471 40 (2015) 9382–9387. <https://doi.org/10.1016/j.ijhydene.2015.05.088>.
- 472 [26] S. Pioquinto-García, J.M. Rosas, M. Loredó-Cancino, S. Giraudet, E. Soto-
473 Regalado, P. Rivas-García, N.E. Dávila-Guzmán, Environmental assessment of
474 metal-organic framework DUT-4 synthesis and its application for siloxane removal,
475 *J. Environ. Chem. Eng.* 9 (2021) 106601. <https://doi.org/10.1016/j.jece.2021.106601>.
- 476 [27] S. Brunauer, P.H. Emmett, E. Teller, Adsorption of Gases in Multimolecular Layers,
477 *J. Am. Chem. Soc.* 60 (1938) 309–319. [https://doi.org/citeulike-article-
478 id:4074706](https://doi.org/citeulike-article-id:4074706) \rdoi: 10.1021/ja01269a023.
- 479 [28] W.D. Harkins, G. Jura, Surfaces of Solids. XIII. A Vapor Adsorption Method for the
480 Determination of the Area of a Solid without the Assumption of a Molecular Area,
481 and the Areas Occupied by Nitrogen and Other Molecules on the Surface of a Solid,
482 *J. Am. Chem. Soc.* 66 (1944) 1366–1373. <https://doi.org/10.1021/ja01236a048>.
- 483 [29] M. Thommes, K. Kaneko, A. V. Neimark, J.P. Olivier, F. Rodriguez-Reinoso, J.
484 Rouquerol, K.S.W. Sing, Physisorption of gases, with special reference to the
485 evaluation of surface area and pore size distribution (IUPAC Technical Report), *Pure
486 Appl. Chem.* 87 (2015) 1051–1069. <https://doi.org/10.1515/pac-2014-1117>.

- 487 [30] G.W. Peterson, D.T. Lee, H.F. Barton, T.H. Epps, G.N. Parsons, Fibre-based
488 composites from the integration of metal–organic frameworks and polymers, *Nat.*
489 *Rev. Mater.* 6 (2021) 605–621. <https://doi.org/10.1038/s41578-021-00291-2>.
- 490 [31] A. DeVierno Kreuder, T. House-Knight, J. Whitford, E. Ponnusamy, P. Miller, N.
491 Jesse, R. Rodenborn, S. Sayag, M. Gebel, I. Aped, I. Sharfstein, E. Manaster, I.
492 Ergaz, A. Harris, L. Nelowet Grice, A Method for Assessing Greener Alternatives
493 between Chemical Products Following the 12 Principles of Green Chemistry, *ACS*
494 *Sustain. Chem. Eng.* 5 (2017) 2927–2935.
495 <https://doi.org/10.1021/acssuschemeng.6b02399>.
- 496 [32] C. Brambila, P. Boyd, A. Keegan, P. Sharma, C. Vetter, E. Ponnusamy, S. V.
497 Patwardhan, A Comparison of Environmental Impact of Various Silicas Using a
498 Green Chemistry Evaluator, *ACS Sustain. Chem. Eng.* 10 (2022) 5288–5298.
499 <https://doi.org/10.1021/acssuschemeng.2c00519>.
- 500 [33] J. Liu, H. Cao, Y. Shi, P. Jiang, Enhanced Methane Delivery in MIL-101(Cr) by
501 Means of Subambient Cooling, *Energy & Fuels.* 35 (2021) 6898–6908.
502 <https://doi.org/10.1021/acs.energyfuels.1c00617>.
- 503 [34] J. Crank, *The Mathematics of Diffusion*, Clarendon Press, Oxford, 1979.
504 <https://books.google.com.mx/books?id=eHANhZwVouYC>.
- 505 [35] M. Armstrong, P. Sirous, B. Shan, R. Wang, C. Zhong, J. Liu, B. Mu, Prolonged
506 HKUST-1 functionality under extreme hydrothermal conditions by electrospinning
507 polystyrene fibers as a new coating method, *Microporous Mesoporous Mater.* 270

- 508 (2018) 34–39. <https://doi.org/10.1016/j.micromeso.2018.05.004>.
- 509 [36] J.F. Kurisingal, Y. Li, Y. Sagynbayeva, R.K. Chitumalla, S. Vuppala, Y. Rachuri, Y.
510 Gu, J. Jang, D.-W. Park, Porous aluminum-based DUT metal-organic frameworks
511 for the transformation of CO₂ into cyclic carbonates: A computationally supported
512 study, *Catal. Today*. 352 (2020) 227–236.
513 <https://doi.org/10.1016/j.cattod.2019.12.038>.
- 514 [37] H. Embrechts, M. Kriesten, M. Ermer, W. Peukert, M. Hartmann, M. Distaso, In situ
515 Raman and FTIR spectroscopic study on the formation of the isomers MIL-68(Al)
516 and MIL-53(Al), *RSC Adv.* 10 (2020) 7336–7348.
517 <https://doi.org/10.1039/C9RA09968A>.
- 518 [38] E. Pretsch, P. Bühlmann, M. Badertscher, IR Spectroscopy, in: *Struct. Determ. Org.*
519 *Compd.*, Springer-Verlag, Berlin, Heidelberg, 2009: pp. 1–67.
520 https://doi.org/10.1007/978-3-540-93810-1_7.
- 521 [39] Y. Zhang, N. Tajaddod, K. Song, M.L. Minus, Low temperature graphitization of
522 interphase polyacrylonitrile (PAN), *Carbon N. Y.* 91 (2015) 479–493.
523 <https://doi.org/10.1016/j.carbon.2015.04.088>.
- 524 [40] X. Hu, D.J. Johnson, J.G. Tomka, Molecular Modelling of the Structure of
525 Polyacrylonitrile Fibres, *J. Text. Inst.* 86 (1995) 322–331.
526 <https://doi.org/10.1080/00405009508631337>.
- 527 [41] S. Lee, J. Kim, B.-C. Ku, J. Kim, H.-I. Joh, Structural Evolution of Polyacrylonitrile
528 Fibers in Stabilization and Carbonization, *Adv. Chem. Eng. Sci.* 02 (2012) 275–282.

- 529 <https://doi.org/10.4236/aces.2012.22032>.
- 530 [42] P. Sharma, C. Vetter, E. Ponnusamy, E. Colacino, Assessing the Greenness of
531 Mechanochemical Processes with the DOZN 2.0 Tool, ACS Sustain. Chem. Eng. 10
532 (2022) 5110–5116. <https://doi.org/10.1021/acssuschemeng.1c07981>.
- 533 [43] J. Kärger, D.M. Ruthven, D.N. Theodorou, Sorption Kinetics, in: Diffus.
534 Nanoporous Mater., Wiley, 2012: pp. 143–189.
535 <https://doi.org/10.1002/9783527651276.ch6>.
- 536 [44] V.T.L. Tran, P. Gélin, C. Ferronato, J. Chovelon, L. Fine, G. Postole, Adsorption of
537 linear and cyclic siloxanes on activated carbons for biogas purification: Sorbents
538 regenerability, Chem. Eng. J. 378 (2019) 122152.
539 <https://doi.org/10.1016/j.cej.2019.122152>.
- 540
- 541

542 **Tables**543 **Table 1.** Details of each electrospinning solution employed.

Notation	Solution 1		Solution 2			Electrospinning operational mode
	PAN (g)	DMF (g)	DUT-4 (g)	DMF (g)	PAN (g)	
PAN	0.3	3.0	N/A ^a	N/A	N/A	Uniaxial
20DUT-4/PAN	0.5	2.0	0.1	3.0	N/A	Uniaxial
20DUT-4@PAN	0.4	2.5	0.1	2.5	0.1	Coaxial
70DUT-4@PAN	0.25	3.0	0.25	3.0	0.1	Coaxial
100DUT-4@PAN	0.25	3.0	0.35	3.0	0.1	Coaxial
140DUT-4@PAN	0.25	3.0	0.50	3.0	0.1	Coaxial

544 ^aN/A: not applicable

545

546 **Table 2.** Textural properties derived from the nitrogen adsorption-desorption isotherms
547 obtained at -196 °C of the DUT-4 fibers.

Fiber notation	S_{BET} (m ² /g)	V_{mp} (cm ³ /g)	S_t (m ² /g)	V_{mes} (cm ³ /g)	V_p (cm ³ /g)
PAN	11	0.002	6	0.025	0.027
20DUT-4/PAN	20	0.004	10	0.055	0.059
20DUT-4@PAN	37	0.010	13	0.090	0.100
70DUT-4@PAN	113	0.033	33	0.188	0.221
100DUT-4@PAN	131	0.040	35	0.120	0.160
140DUT-4@PAN	293	0.100	51	0.264	0.363

548

549 **Table 3.** Kinetic model parameters for siloxane D4 adsorption.

550

Adsorbent	PS-1		PS-2		Crank	
	K_1 (h ⁻¹)	R^2	K_2 (h ⁻¹)	R^2	D (m ² /h)	R^2
DUT-4	1.14	0.9456	0.22	0.9231	1.76×10^{-8}	0.9768
20DUT-4/PAN	6.43	0.9917	2.13	0.9977	4.22×10^{-8}	0.9921
20DUT-4@PAN	5.87	0.9671	1.18	0.9840	5.12×10^{-8}	0.9780
70DUT-4@PAN	5.33	0.8810	0.76	0.9736	5.82×10^{-8}	0.9530
100DUT-4@PAN	2.59	0.9692	0.61	0.9463	3.32×10^{-8}	0.9823

140DUT-4@PAN	2.59	0.9460	0.38	0.9860	3.32×10^{-8}	0.9936
--------------	------	--------	------	--------	-----------------------	--------

551

Journal Pre-proof

552 **Figure captions**

553 **Fig. 1.** Crystal structure of DUT-4. (A) the aluminum octahedra are linked by NDC groups,
554 (B) view of the rectangular tunnels ($9 \text{ \AA} \times 9 \text{ \AA}$) along the [010] direction. Color code: gray,
555 C; red, O; blue polyhedral, Al.

556 **Fig. 2.** Nitrogen adsorption-desorption isotherms obtained at $-196 \text{ }^\circ\text{C}$ of the DUT-4 fibers
557 prepared by uniaxial (a) and coaxial (b) electrospinning configuration at different
558 experimental conditions.

559 **Fig. 3.** SEM micrographs of electrospun fibers: (A) PAN, (B) 20DUT-4/PAN, (C) 20DUT-
560 4@PAN, (D) 70DUT-4@PAN, (E) 100DUT-4@PAN, (F) 140DUT-4@PAN.

561 **Fig. 4.** ATR-FTIR spectra of the pristine DUT-4 and the fibers (PAN and 70DUT-
562 4@PAN).

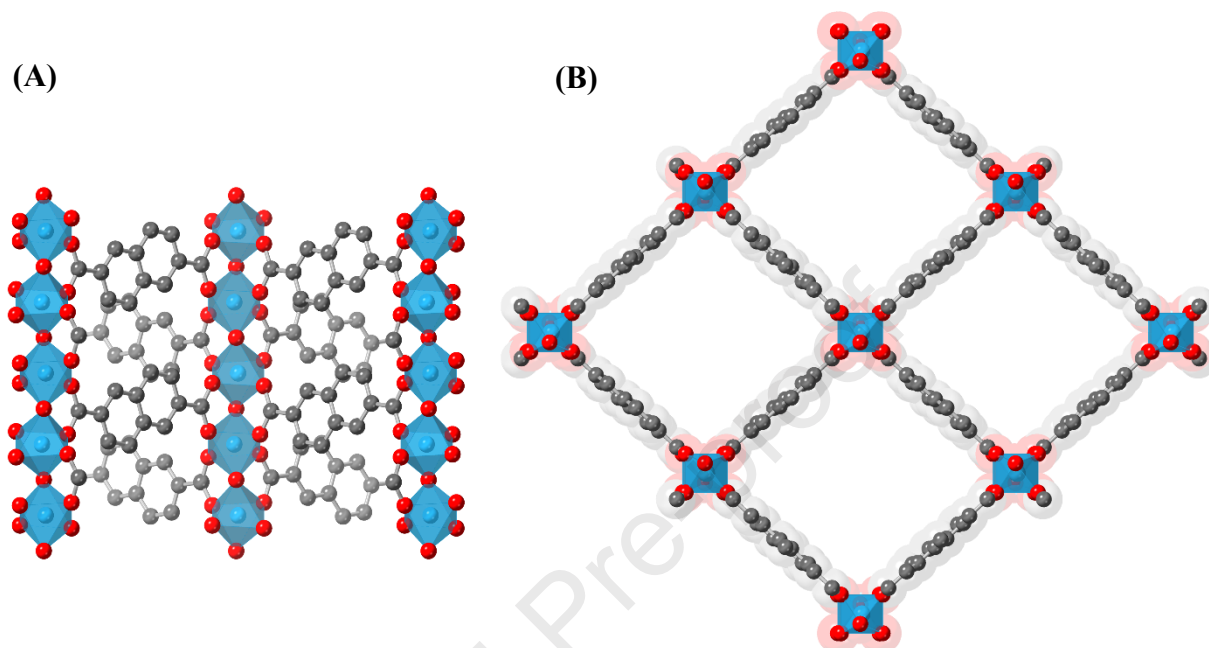
563 **Fig. 5.** PXRD patterns of (a) simulated DUT-4, (b) as-synthesized DUT-4 powders, (c)
564 electrospun DUT-4 powders-embedded fibers (70DUT-4@PAN), and (d) PAN fibers. The
565 insert presents the chain packing of PAN in [110] direction.

566 **Fig. 6.** (A) TGA and (B) DTG curves of PAN and 70DUT-4@PAN fibers.

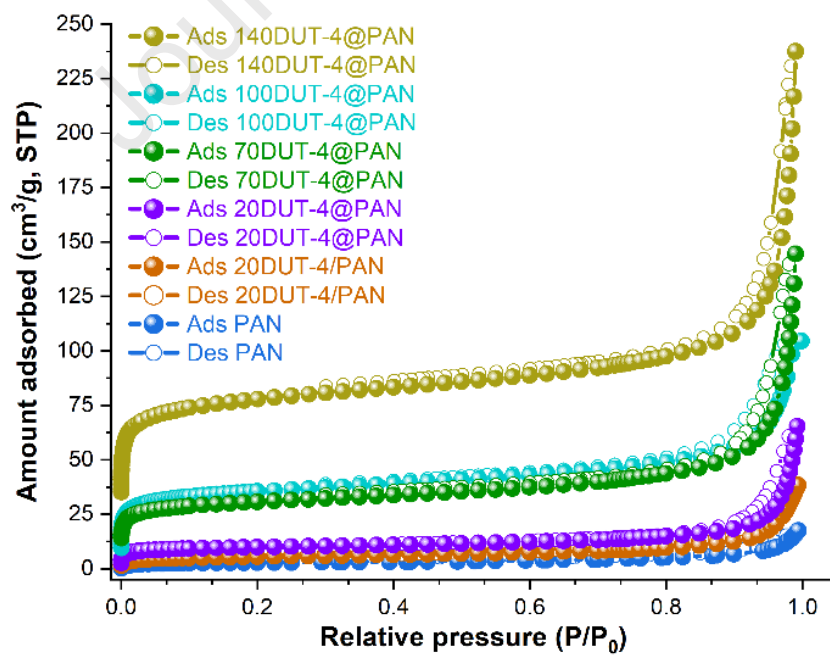
567 **Fig. 7.** Green Assessment of DUT-4 and 70DUT-4@PAN.

568 **Fig. 8.** Adsorption kinetics profiles of electrospun DUT-4 fibers at room temperature and
569 initial D4 concentration of 450 mg/Nm^3 .

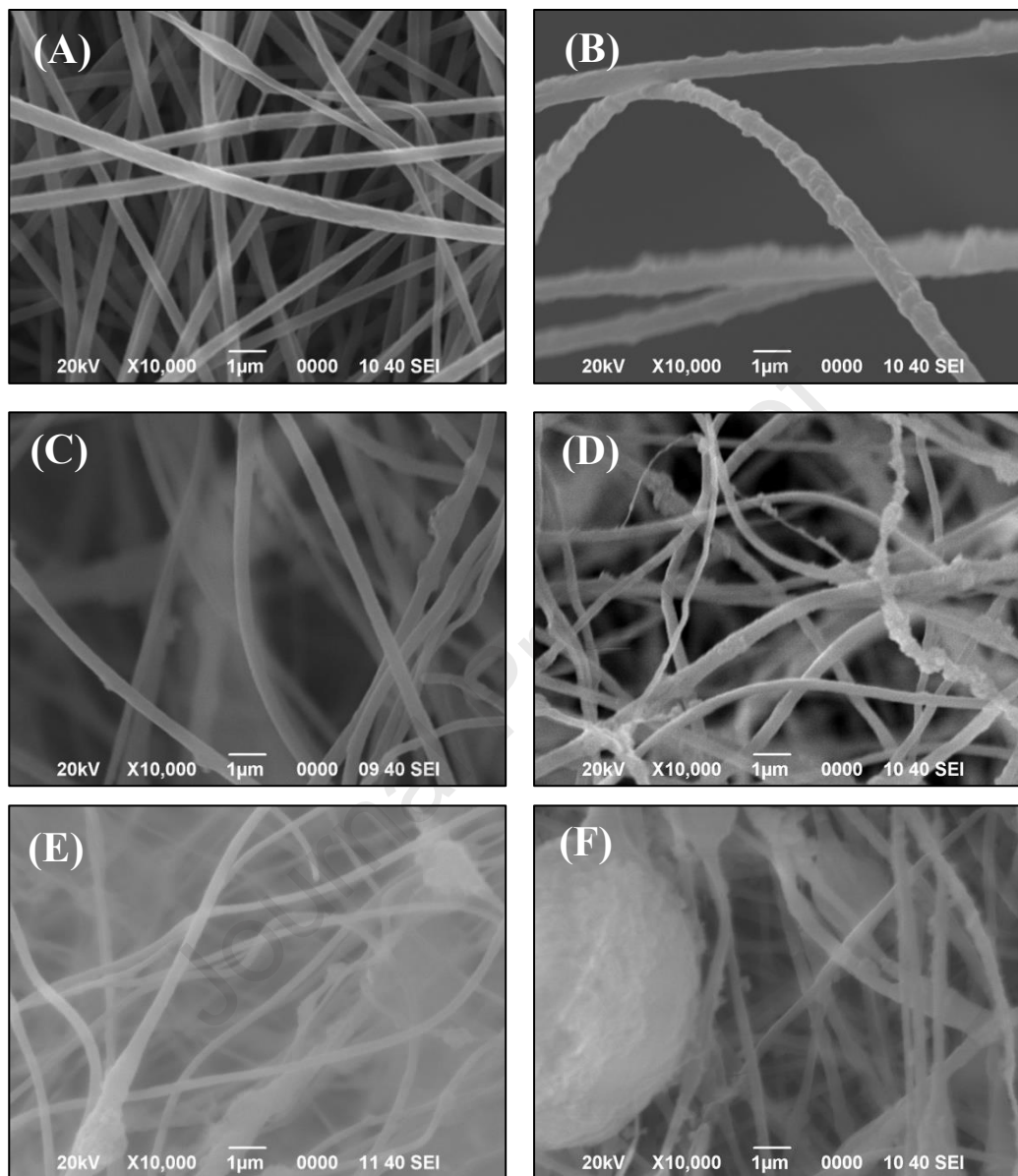
570 **Fig. 9.** Effective diffusion coefficients for D4 siloxane adsorption at 450 mg/Nm^3 and room
571 temperature.

572 **Figures**573 **Figure 1**

574

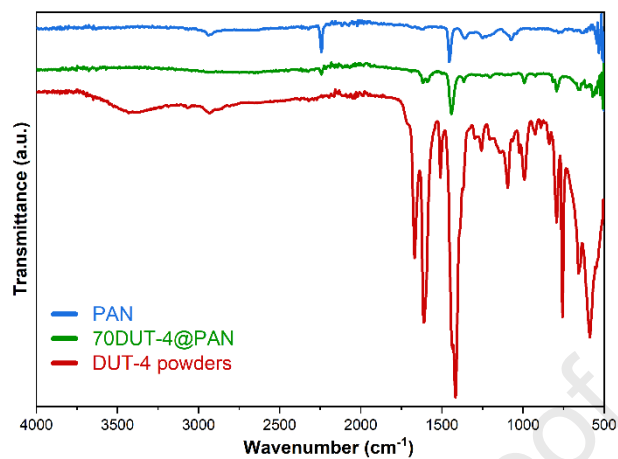
575 **Figure 2**

576

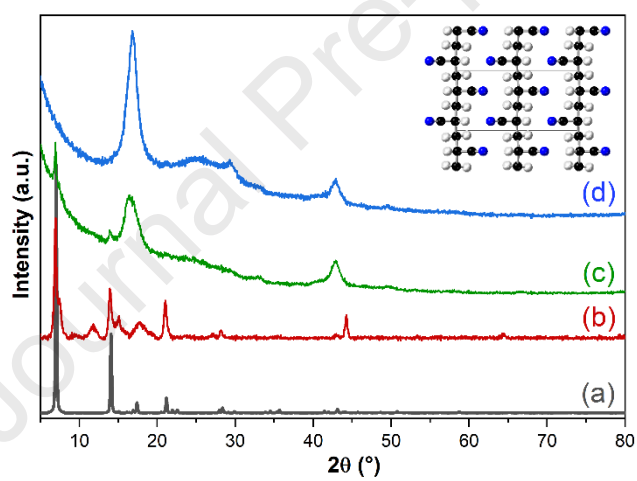
577 **Figure 3**

578

579

580 **Figure 4**

581

582 **Figure 5**

583

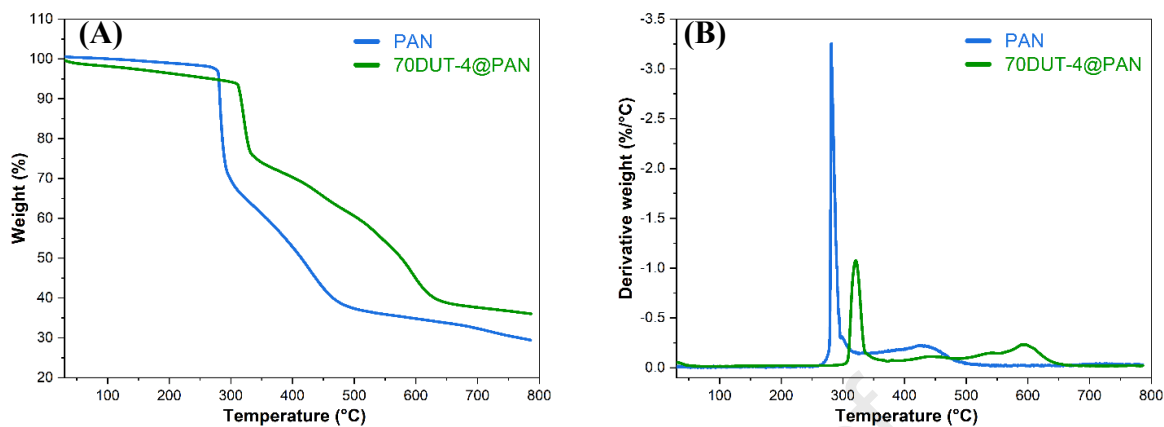
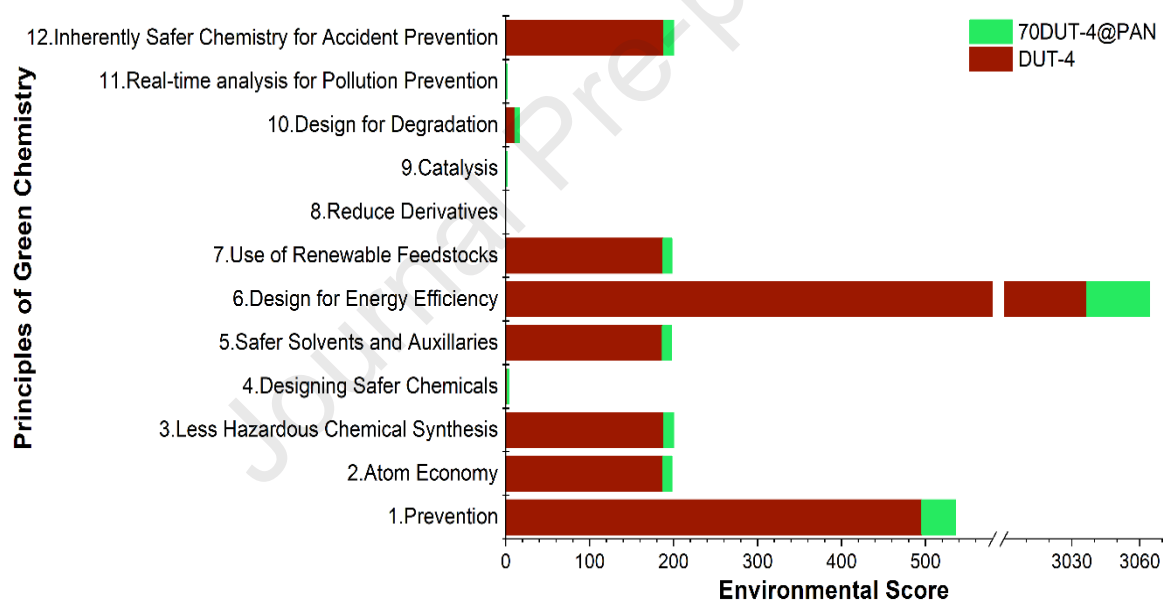
584

585

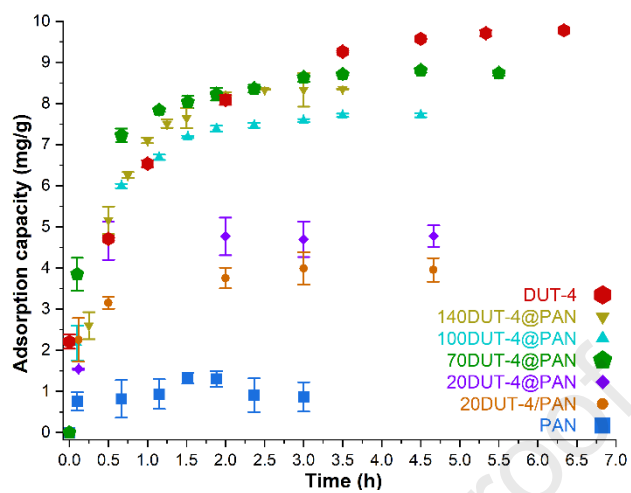
586

587

588

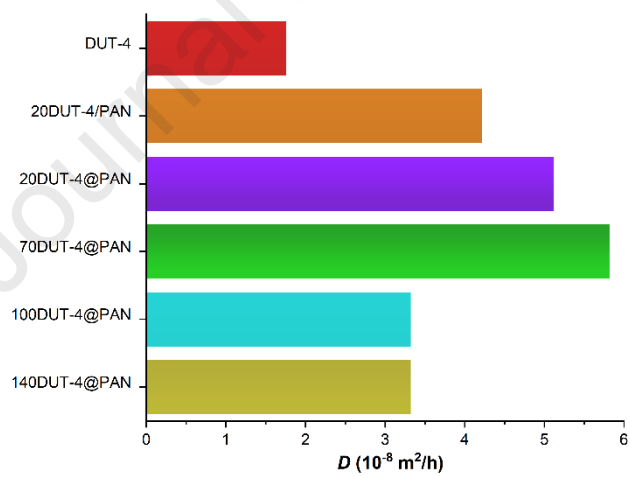
589 **Figure 6**590
591592 **Figure 7**

593

594 **Figure 8**

595

596

597 **Figure 9**

598

- Aluminum-based MOF/PAN composite fibers were prepared by electrospinning
- Coaxial electrospun fibers show superior textural characteristics
- The fibers can be used to adsorb siloxane D4 at low concentrations
- 70DUT-4@PAN has the best relation between adsorption kinetics/environmental impact

Journal Pre-proof

Declaration of interests

The authors declare that they have no known competing financial interests or personal relationships that could have appeared to influence the work reported in this paper.

The authors declare the following financial interests/personal relationships which may be considered as potential competing interests:

Journal Pre-proof